

Slow magnetic relaxation in two mononuclear Mn(II) complexes not governed by the over-barrier Orbach process

R. Mičová, C. Rajnák, J. Titiš, E. Samoľová, M. Zalibera, A. Bieńko, R. Boča

Supplementary Information

Physical Measurements. FT-IR spectra were measured by ATR method in region $400 - 4000 \text{ cm}^{-1}$ at room temperature (Shimadzu IRAffinity-1, Quest ATR holder). Absorption spectra in the UV–Vis region ($9000 - 50\,000 \text{ cm}^{-1}$) were recorded by UV–Vis–NIR spectrophotometer (Varian, 50 Bio). Electronic spectra of powdered samples in Nujol oil were recorded at room temperature in region $9000 - 50\,000 \text{ cm}^{-1}$ (Specord 200, Analytical Jena). X-band cw-EPR spectra (9.5 GHz) were obtained with portable X-Band EPR spectrometer PS 100X (Adani, Belarus) equipped with the $\text{N}_2(\text{l})$ "finger-dewar". Powder samples of the complex were filled into 4 mm diameter quartz tubes and the spectra were recorded at 298 K and 77 K. EPR spectra were simulated using the Easyspin toolbox, running under the Matlab platform.¹ Magnetic data in the DC and AC modes were taken using the SQUID magnetometer (MPMS-XL5, Quantum Design). The sample was encapsulated in a diamagnetic gelatin cup. The DC data was collected at $B_{DC} = 0.5 \text{ T}$ and corrected to the underlying diamagnetism. Magnetization data was taken at $T = 2.0$ and 5 K up to $B_{DC} = 5 \text{ T}$. Small oscillating magnetic field with amplitude $B_{AC} = 0.3 \text{ mT}$ was used in taking the AC susceptibility data as functions of the frequency $f = 1$ to 1500 Hz, external magnetic field B_{DC} , and temperature.

\$ X-ray structure analysis. The single-crystal X-ray diffraction studies for compound **1** were carried out on a 4-circle diffractometer Stoe Stadivari with Xenocs Genix3D Cu HF microfocused X-ray source ($\text{CuK}\alpha$ radiation, $\lambda = 1.54186 \text{ \AA}$) equipped with Dectris Pilatus3R 300K detector. The data were integrated, reduction and scaled using the Stoe X-Area program and absorption correction were made multi-scan method using Stoe LANA software. The structure was solved with the Sir-2014 solution program and refined with ShelXL-2018/3 using full-matrix least-squares minimization on F^2 . Bruker D8-Venture 3-circle diffractometer equipped with a Photon3 detector and MoK α radiation ($\lambda = 0.7107 \text{ \AA}$) for compound **2**. Data were collected using ϕ and ω scans in a nitrogen gas stream at 100 K. The data were integrated using the Bruker SAINT Software program and scaled using the SADABS software program. The structure was solved with the ShelXT solution program using dual methods and by using Olex2 1.5-alpha as the graphical interface. The model was refined with XL using full-matrix least-squares minimization on F^2 . All nonhydrogen atoms were refined anisotropically by full-matrix least-squares. All carbon bonded hydrogen atoms were placed using a riding model. Their positions were constrained relative to their parent atom using the appropriate HFIX command in SHELLXL-2014.²⁻⁶

† *Ab initio* calculations were performed with ORCA 5.0.3 computational package using the experimental geometry of complexes under study.^{7,8} The relativistic effects were included in the calculations with zero-order regular approximation (ZORA) together with the scalar relativistic contracted version of def2-TZVPP basis functions for Mn, O and N atoms, def2-SV(P) basis function for other elements. The calculations of ZFS parameters were based on state average complete active space self-consistent field (SA-CASSCF) wave functions complemented by N-electron valence second order perturbation theory (NEVPT2).⁹⁻¹² The active space of the CASSCF calculations comprised of five electrons in five metal-based d-orbitals. The state averaged approach was used, in which all 1 sextet, 24 quartet and 75 doublet states were equally weighted. The calculations utilized the RI approximation with appropriate decontracted auxiliary basis set and the chain-of-spheres (RIJCOSX) approximation to exact exchange. Increased integration grids (Grid4 and GridX5) and tight SCF convergence criteria were used. The ZFS parameters were calculated through quasi-degenerate perturbation theory in which an approximation to the Breit-Pauli form of the spin-orbit coupling operator (SOMF) and the effective Hamiltonian theory was utilized.¹³⁻¹⁵ Relative energies and shapes of singly occupied molecular orbitals were calculated using the *ab initio* ligand-field theory (AI-LFT).¹⁶

1 S. Stoll, A. Schweiger, *Journal of Magnetic Resonance*, 2006, **178**, 42.

2 O. V. Dolomanov, L. J. Bourhis, R. J. Gildea, J. A. K. Howard, H. Puschmann, *J. Appl. Cryst.*, 2009, **42**, 339-341.

3 G. M. Sheldrick, *Acta Cryst.*, 2015, **C71**, 3-8.

4 G. M. Sheldrick, *Acta Cryst.*, 2015, **A71**, 3-8.

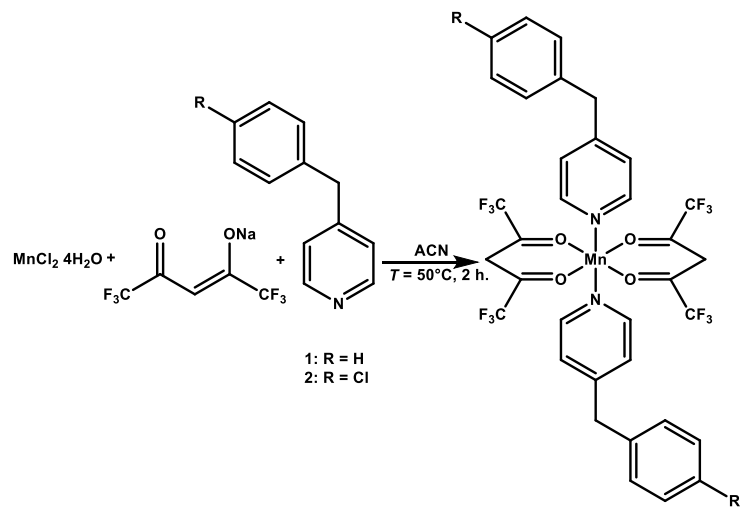
Slow magnetic relaxation in two mononuclear Mn(II) complexes not governed by the over-barrier Orbach process

R. Mičová, C. Rajnák, J. Titiš, E. Samoľová, M. Zalibera, A. Bieńko, R. Boča

- 5 J. Krause, R. Herbst-Irmer, G. M. Sheldrick, D. Stalke, *J. Appl. Cryst.*, 2015, **48**, 3-10.
- 6 J. Kožíšková, F. Hahn, J. Richter, J. Kožíšek, *Acta Chimica Slovaca*, 2016, **9**, 136 - 140.
- 7 F. Neese, *WIREs Comput. Mol. Sci.*, 2012, **2**, 73-78.
- 8 F. Neese, ORCA – An Ab Initio, Density Functional and Semi-empirical Program Package, Version 4.2.1.
- 9 M. Atanasov, D. Ganyushin, D. A. Pantazis, K. Sivalingam and F. Neese, *Inorg. Chem.*, 2011, **50**, 7460-7477.
- 10 C. Angeli, S. Borini, M. Cestari and R. Cimiraglia, *J. Chem. Phys.*, 2004, **121**, 4043-4049.
- 11 C. Angeli, R. Cimiraglia, S. Evangelisti, T. Leininger and J.-P Malrieu, *J. Chem. Phys.*, 2001, **114**, 10252-10264.
- 12 C. Angeli, R. Cimiraglia and J.-P. Malrieu, *J. Chem. Phys.*, 2002, **117**, 9138-9153.
- 13 F. Neese, *J. Chem. Phys.*, 2005, **122**, 34107-34119.
- 14 D. Ganyushin and F. Neese, *J. Chem. Phys.*, 2006, **125**, 24103.
- 15 F. Neese, *J. Chem. Phys.*, 2007, **127**, 164112-164119.
- 16 M. Atanasov, D. Ganyushin, K. Sivalingam, F. Neese, in Molecular Electronic Structures of Transition Metal Complexes II (eds. D. M. P. Mingos, P. Day, J. P. Dahl,), 2011 (Springer Berlin Heidelberg) 149-220.

Chemical synthesis

Complexes were prepared following the synthetic route in Scheme 1. The organic reactants (4-benzylpyridine, 4-(4-chlorobenzyl)pyridine), inorganic salt $\text{MnCl}_2 \cdot 4\text{H}_2\text{O}$ and sodium hexafluoroacetylacetone of reagent grade were purchase and used as received. Acetonitrile was not dried and used without any further purification.



Scheme S1. Synthetic route of **1** and **2**.

Preparation of the complex $[\text{Mn}(4\text{-ppy})_2(\text{hfa})_2]$ (**1**).

Sodium hexafluoroacetylacetone (1 mmol, 0.230 g) was dissolved in acetonitrile (15 cm³) and afterwards manganese(II) chloride tetrahydrate (0.5 mmol, 0.0989 g) was added. The mixture was stirred for 15 min. and 4-benzylpyridine (4-ppy) (1.5 mmol, 0.239 cm³) was added. The resulting mixture was stirred and heated under reflux for 2 hours. After refluxing, the solution was filtered off and left for crystallization. The yellow-orange crystals were collected after 5 days. Yield: 55% (0.245 g). Melting point: 152°C. *Anal. Calc.* for $\text{C}_{34}\text{H}_{24}\text{F}_{12}\text{MnN}_2\text{O}_4$ ($M = 807.49 \text{ g} \cdot \text{mol}^{-1}$): C, 50.57; H, 3.00; N, 3.47. Found: C, 50.27; H, 2.85; N, 3.71. Selected IR bands / (cm⁻¹): 1643 $\nu_{\text{as}}(\text{C-C})$, 1615 $\nu_{\text{s}}(\text{C-O})$, 1256 $\nu_{\text{s}}(\text{C-C})$ 1203 $\nu_{\text{as}}(\text{CF}_3)$, 1180 $\nu_{\text{s}}(\text{CF}_3)$ 1134 (C-H), 795 (C-CF₃). UV/Vis (Nujol) $\nu_{\text{max}}/10^3 \text{ cm}^{-1}$ (relat. absorb.): 32.

Slow magnetic relaxation in two mononuclear Mn(II) complexes not governed by the over-barrier Orbach process

R. Mičová, C. Rajnák, J. Titiš, E. Samoľová, M. Zalibera, A. Bieńko, R. Boča

Preparation of the complex $[\text{Mn}(\text{4-ppyCl})_2(\text{hfa})_2]$ (**2**).

Sodium hexafluoroacetylacetone (1 mmol, 0.230 g) was dissolved in acetonitrile (15 cm³) and afterwards manganese(II) chloride tetrahydrate (0.5 mmol, 0.0989 g) was added. The mixture was stirred for 15 min. and 4-(4-chlorobenzyl)pyridine (4-ppyCl) (1.5 mmol, 0.263 cm³) was added. The resulting mixture was stirred and heated under reflux for 2 hours. After refluxing, the solution was filtered off and left for crystallization. The yellow-orange crystals were collected after 5 days. Yield: 52% (0.25 g). Melting point: 136°C. Selected IR bands / (cm⁻¹): 1645 $\nu_{\text{as}}(\text{C-C})$, 1610 $\nu_{\text{s}}(\text{C-O})$, 1256 $\nu_{\text{s}}(\text{C-C})$, 1196 $\nu_{\text{s}}(\text{CF}_3)$, 1131 (C-H), 789 (C-CF₃). UV/Vis (ACN) $\nu_{\text{max}}/10^3 \text{ cm}^{-1}$ ($c = 1.05 \cdot 10^{-4} \text{ mol} \cdot \text{dm}^3$): 32.21 (2.325; $\varepsilon = 22\,149 \text{ M}^{-1} \cdot \text{cm}^{-1}$).

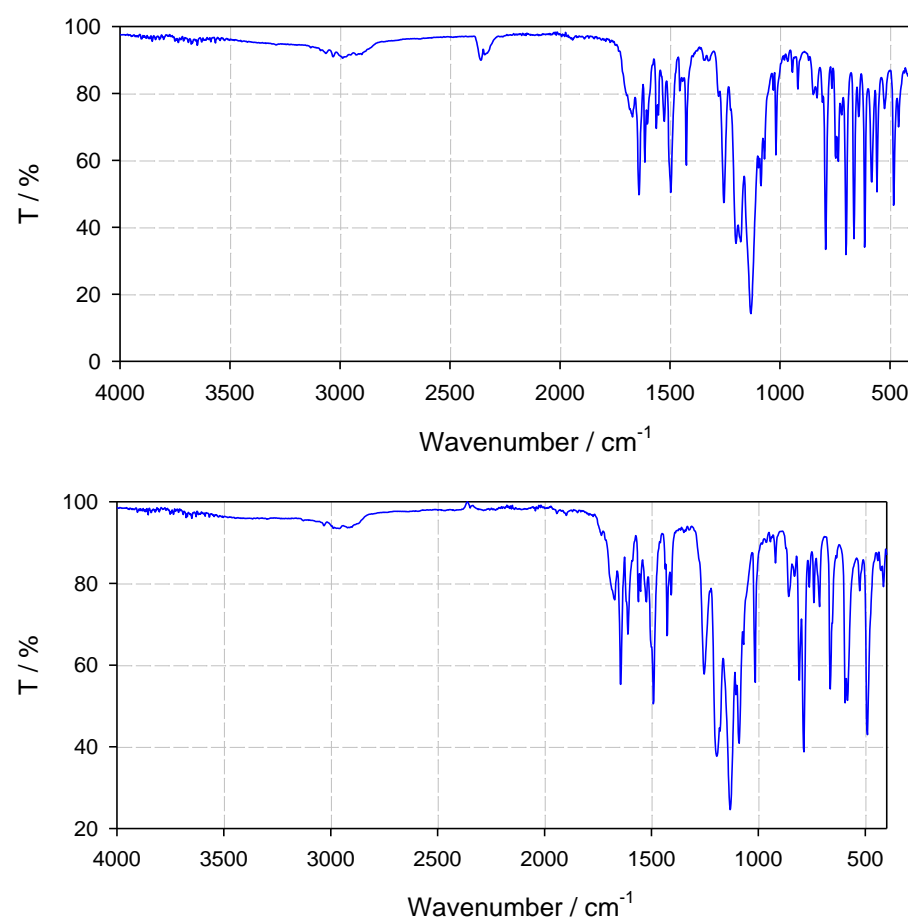


Figure S1. IR spectra of $[\text{Mn}^{\text{II}}(\text{4-ppy})_2(\text{hfa})_2]$, **1**, (top) and $[\text{Mn}^{\text{II}}(\text{4-ppyCl})_2(\text{hfa})_2]$, **2** (bottom).

Slow magnetic relaxation in two mononuclear Mn(II) complexes not governed by the over-barrier Orbach process

R. Mičová, C. Rajnák, J. Titiš, E. Samoľová, M. Zalibera, A. Bieńko, R. Boča

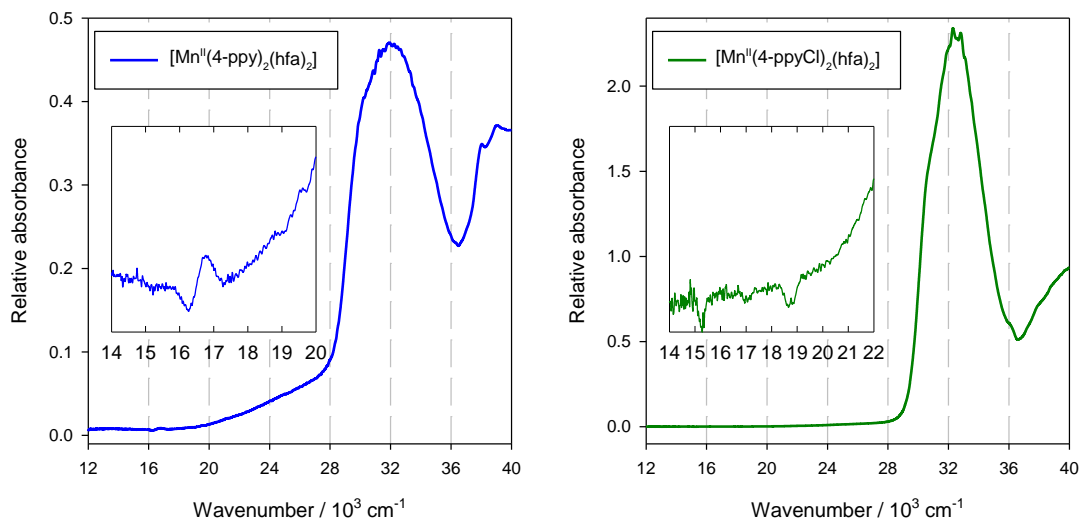


Figure S2. Electronic spectrum of **1** and **2**. Bands at $32\ 000\ \text{cm}^{-1}$ are typical for ${}^6\text{A}_{1(\text{g})}$ to ${}^4\text{T}_{1(\text{g})}(\text{P})$ transitions.

Slow magnetic relaxation in two mononuclear Mn(II) complexes not governed by the over-barrier Orbach process

R. Mičová, C. Rajnák, J. Titiš, E. Samoľová, M. Zalibera, A. Bieňko, R. Boča

Table S1. Crystal data and structure refinement parameters of **1** and **2**.

	[Mn ^{II} (4-ppy) ₂ (hfa) ₂], 1	[Mn ^{II} (4-ppyCl) ₂ (hfa) ₂], 2
Empirical formula	C ₃₄ H ₂₄ F ₁₂ MnN ₂ O ₄	C ₃₄ H ₂₂ Cl ₂ F ₁₂ MnN ₂ O ₄
Formula weight	807.49	876.37
Temperature/K	100	100
Crystal system	Monoclinic	Monoclinic
Space group	P2 ₁ /n	P2 ₁ /n
a/Å	9.1007(3)	9.0957(12)
b/Å	18.3155(6)	14.6737(14)
c/Å	10.1535(4)	14.2674(17)
α°	90	90
β°	99.269(3)	107.613(5)
γ°	90	90
Volume/Å ³	1670.33(10)	1815.0(4)
Z	2	2
ρ_{calc} g/cm ³	1.606	1.604
μ/mm^{-1}	4.216	0.614
F(000)	814.0	878
Crystal size/mm ³	0.25 × 0.16 × 0.08	0.25 × 0.22 × 0.20
Radiation	Cu K α ($\lambda = 1.54186$)	Mo K α ($\lambda = 0.71073$)
2 Θ range for data collection/ $^{\circ}$	9.658 to 143.772	5.458 to 51.45
Index ranges	-10 ≤ h ≤ 10, -14 ≤ k ≤ 21, -10 ≤ l ≤ 12	-11 ≤ h ≤ 11, -17 ≤ k ≤ 17, -17 ≤ l ≤ 17
Reflections collected	14594	39485
Independent reflections	3181 [R _{int} = 0.0280, R _{sigma} = 0.0217]	3443 [R _{int} = 0.0429, R _{sigma} = 0.0185]
Data/restraints/parameters	3181/0/241	3443/162/324
Goodness-of-fit on F2	1.037	1.051
Final R indexes [I>=2σ (I)]	R ₁ = 0.0351, wR ₂ = 0.0891	R ₁ = 0.0279, wR ₂ = 0.0617
Final R indexes [all data]	R ₁ = 0.0427, wR ₂ = 0.0936	R ₁ = 0.0345, wR ₂ = 0.0646
Largest diff. peak/hole / e Å ⁻³	0.25/-0.36	0.255/-0.278
Colour	Yellow orange	Yellow orange
CCDC	2167772	2167775

Table S2. Bond lengths (\AA) and bond angles (deg) within the coordination polyhedron of **1** and **2**.

1	2						
M-L	X-Mn-Y		M-L	X-Mn-Y			
Mn-O1	2.1555(13)	O1-Mn1-O1 ¹	180.0	Mn-O1	2.1577(11)	O1-Mn1-O2 ¹	95.00(4)
Mn-O2	2.1532(13)	O1 ¹ -Mn1-N1 ¹	91.15(5)	Mn1-O2	2.1644(10)	O1 ¹ -Mn1-N1 ¹	91.92(4)
Mn-N1	2.2508(16)	O1-Mn1-N1	91.15(5)	Mn1-N1	2.2529(13)	O1-Mn1-O1	180.00
<i>d</i> _{av} (M-N)	2.2508	O1-Mn1-N1 ¹	88.85(5)	<i>d</i> _{av} (M-N)	2.2528	O1-Mn1-O2	85.00(4)
<i>d</i> _{av} (M-O)	2.1544	O1 ¹ -Mn1-N1	88.85(5)	<i>d</i> _{av} (M-O)	2.1611	O1 ¹ -Mn1-N1	88.08(4)
		O2-Mn1-O1 ¹	95.00(5)			O2-Mn1-N1 ¹	90.33(4)
		O2 ¹ -Mn1-O1 ¹	85.00(5)			O2 ¹ -Mn1-O1 ¹	85.01(4)
		O2-Mn1-O1	85.00(5)			O2-Mn1-O2	180.00
		O2 ¹ -Mn1-O1	95.00(5)			O2 ¹ -Mn1-O1	95.00(4)
		O2-Mn1-O2 ¹	180.0			N1-Mn1-O1 ¹	88.08(4)
		O2 ¹ -Mn1-N1	91.52(5)			N1-Mn1-O2	89.67(4)
		O2-Mn1-N1	88.48(5)			N1-Mn1-N1	180.00
		O2 ¹ -Mn1-N1 ¹	88.48(5)			O1-Mn1-O2	85.00(4)
		O2-Mn1-N1 ¹	91.52(5)			O1-Mn1-N1 ¹	88.08(4)
		N1-Mn1-N1 ¹	180.0			O2-Mn1-N1 ¹	90.33(4)

Slow magnetic relaxation in two mononuclear Mn(II) complexes not governed by the over-barrier Orbach process

R. Mičová, C. Rajnák, J. Titiš, E. Samoľová, M. Zalibera, A. Bieńko, R. Boča

Table S3. Survey of structural features for **1** and **2** in comparison with **3**.

Complex	Chromo-phore	SHAPE agreement factor ^a					Isomer
		HP-6 (D6h)	PPY-6 (C5v)	OC-6 (Oh)	TPR-6 (D3h)	JPPY-6 (J2)	
1 [Mn ^{II} (4-ppy) ₂ (hfa) ₂]	{MnN ₂ O ₄ }	30.407	28.822	0.188	16.267	32.023	trans
2 [Mn ^{II} (4-ppyCl) ₂ (hfa) ₂]	{MnN ₂ O ₄ }	30.574	28.878	0.184	16.124	32.074	trans
3 [Mn ^{II} (4-bzpy) ₄ Cl ₂]	{MnO ₄ Cl ₂ }	31.732	29.271	0.222	16.457	32.429	trans

^a HP-6 (Hexagon); PPY-6 (Pentagonal pyramid); OC-6 (Octahedron); TPR-6 (Trigonal prism); JPPY-6 (Johnson pentagonal pyramid).

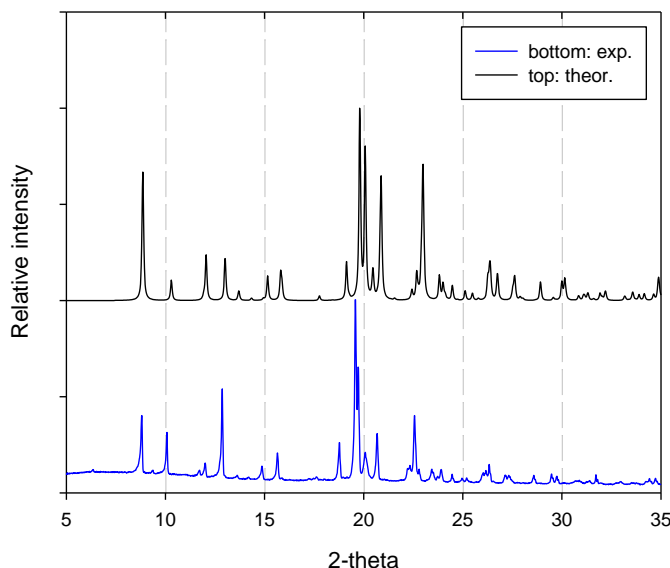
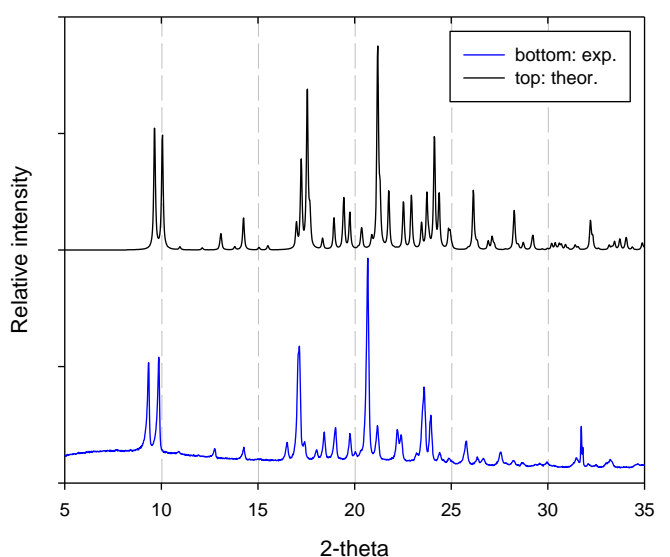


Figure S3. Calculated powder diffraction pattern for **1** and **2** from cif-file (theor.), and recorded pattern at Cu $\lambda = 1.54060 \text{ \AA}$ (exp.).

Slow magnetic relaxation in two mononuclear Mn(II) complexes not governed by the over-barrier Orbach process

R. Mičová, C. Rajnák, J. Titiš, E. Samoľová, M. Zalibera, A. Bieńko, R. Boča

DC magnetic data

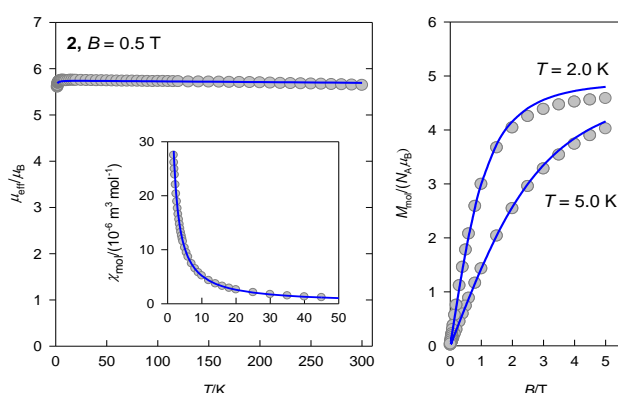


Figure S4. DC magnetic functions for **2**: left – temperature dependence of effective magnetic moment and molar susceptibility; right – field dependence of the magnetization per formula unit. Solid lines – fitted.

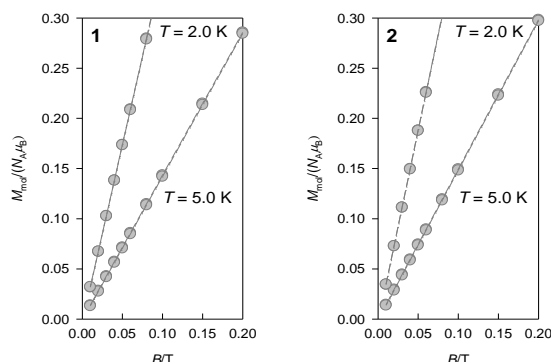


Figure S5. Low-field magnetization data on sweeping the field up and down. The data are identical; there is no indication for the remnant magnetization.

Table S4. Magnetic parameters from the DC magnetic data.^a

	1	2	[Mn ^{II} (4-bzpy) ₄ Cl ₂] ^b
$D/hc / \text{cm}^{-1}$	0.84(13)	0.02	0.95(12)
g_{iso}	2.01(1)	1.95(1)	1.99(1)
$\chi_{\text{TIM}} / 10^{-9} \text{ m}^3 \text{ mol}^{-1} [\text{SI}]$	2.98	-3.0	-1.54
$zj/hc / \text{cm}^{-1}$	-0.0055	-0.0019	-0.0014
$R(\chi)$	0.0043	0.018	0.0026
$R(M)$	0.044	0.034	0.040

^a χ_{TIM} – temperature independent magnetism that compensated uncertainties in the estimation of the underlying diamagnetism and the temperature independent paramagnetism (either positive or negative).

^b Magnetic data from Ref.⁵⁰

Slow magnetic relaxation in two mononuclear Mn(II) complexes not governed by the over-barrier Orbach process

R. Mičová, C. Rajnák, J. Titiš, E. Samoľová, M. Zalibera, A. Bieńko, R. Boča

AC susceptibility data

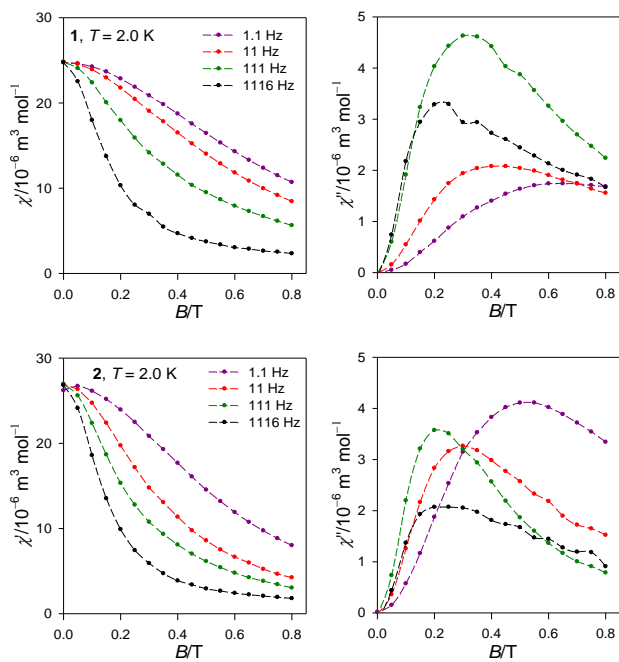


Figure S6. Field dependence of the AC susceptibility for a set of trial frequencies.

Slow magnetic relaxation in two mononuclear Mn(II) complexes not governed by the over-barrier Orbach process

R. Mičová, C. Rajnák, J. Titiš, E. Samoľová, M. Zalibera, A. Bieńko, R. Boča

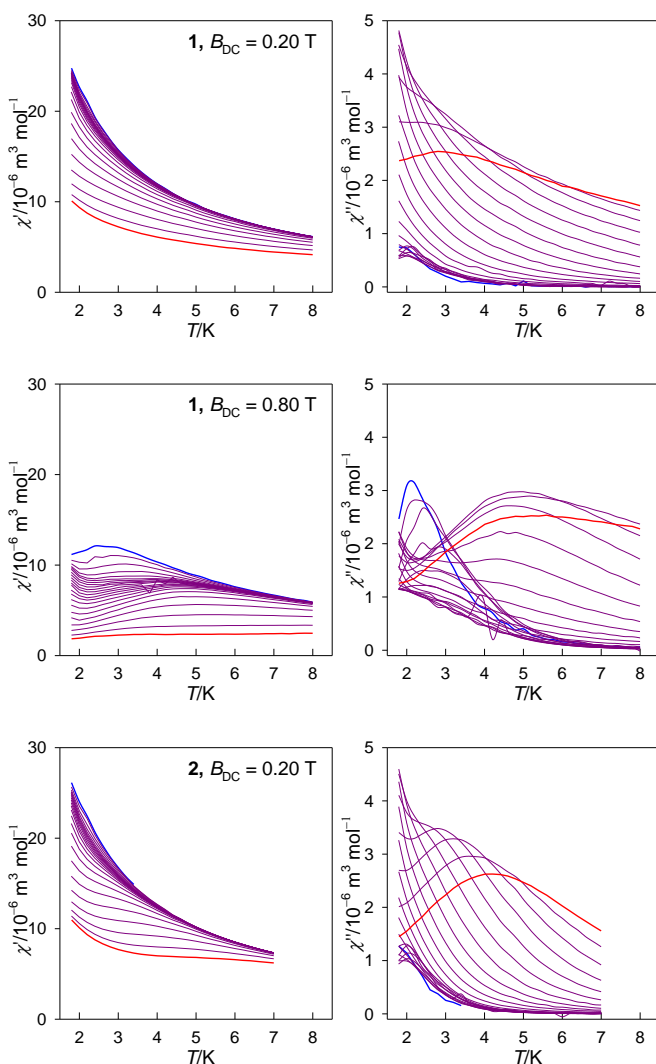


Figure S7. Temperature dependence of the AC susceptibility for **1** and **2**. Blue – the lowest frequency 0.1 Hz, red – the highest 1488 Hz, violet – in between.

Slow magnetic relaxation in two mononuclear Mn(II) complexes not governed by the over-barrier Orbach process

R. Mičová, C. Rajnák, J. Titiš, E. Samoľová, M. Zalibera, A. Bieňko, R. Boča

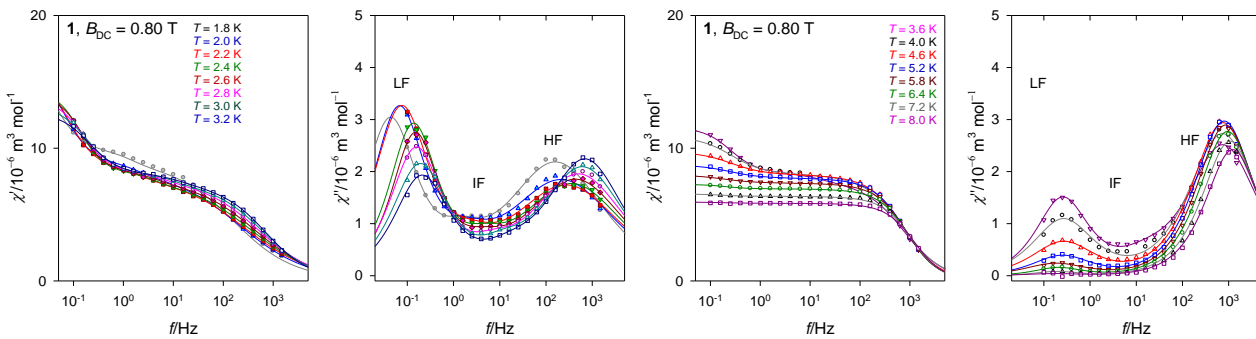


Figure S8. Frequency dependence of the AC susceptibility for **1** split into two windows for clarity.

The AC susceptibility data was fitted by employing the extended Debye equation

$$\chi(\omega) = \chi_s + \sum_k^K \frac{\chi_k - \chi_{k-1}}{1 + (i\omega\tau_k)^{1-\alpha_k}}$$

adapted for the two/three set relaxation channels. For instance, for the two-set case the in-phase and out-of-phase susceptibilities are expressed as

$$\begin{aligned} \chi'(\omega) &= \chi_s + (\chi_{T1} - \chi_s) \frac{1 + (\omega\tau_1)^{1-\alpha_1} \sin(\pi\alpha_1 / 2)}{1 + 2(\omega\tau_1)^{1-\alpha_1} \sin(\pi\alpha_1 / 2) + (\omega\tau_1)^{2-2\alpha_1}} \\ &\quad + (\chi_{T2} - \chi_{T1}) \frac{1 + (\omega\tau_2)^{1-\alpha_2} \sin(\pi\alpha_2 / 2)}{1 + 2(\omega\tau_2)^{1-\alpha_2} \sin(\pi\alpha_2 / 2) + (\omega\tau_2)^{2-2\alpha_2}} \\ \chi''(\omega) &= (\chi_{T1} - \chi_s) \frac{(\omega\tau_1)^{1-\alpha_1} \cos(\pi\alpha_1 / 2)}{1 + 2(\omega\tau_1)^{1-\alpha_1} \sin(\pi\alpha_1 / 2) + (\omega\tau_1)^{2-2\alpha_1}} \\ &\quad + (\chi_{T2} - \chi_{T1}) \frac{(\omega\tau_2)^{1-\alpha_2} \cos(\pi\alpha_2 / 2)}{1 + 2(\omega\tau_2)^{1-\alpha_2} \sin(\pi\alpha_2 / 2) + (\omega\tau_2)^{2-2\alpha_2}} \end{aligned}$$

Table S5. Temperature dependence of AC susceptibility parameters for **1** at $B_{DC} = 0.8$ T.

T/K	$R(\chi')$ %/	$R(\chi'')$ %	χ_{LF}	α_{LF}	τ_{LF} / s	χ_{IF}	α_{IF}	τ_{IF} / 10^{-3} s	χ_{HF}	α_{HF}	τ_{HF} / 10^{-3} s	X_{LF}	X_{IF}	X_{HF}
1.8	2.8	2.9	6.8	.09	3.7	7.7	.0	106	16.7	.42	0.97	.41	.05	.54
2.0	0.83	2.4	7.2(8)	.09	2.4(3)	8.0(6)	.02	75(16)	16.2(7)	.47	0.73(5)	.45	.05	.51
2.2	0.98	1.9	7.8(8)	.12	2.1(2)	8.4(6)	.01	63(16)	16.2(6)	.47	0.57(4)	.48	.04	.49
2.4	0.40	2.3	6.1(2)	.05	1.2(1)	6.8(1)	.01	37(4)	24.4(1)	.44	0.43(2)	.42	.05	.53
2.6	0.63	2.1	5.6(2)	.03	1.1(0)	6.4(2)	.07	36(5)	13.9(1)	.43	0.36(2)	.40	.06	.54
2.8	0.84	1.7	5.5(2)	.09	1.0(1)	6.2(2)	.01	23(4)	13.7(2)	.40	0.31(1)	.40	.04	.55
3.0	0.85	2.2	5.1(2)	.12	0.85(3)	5.8(2)	.03	15(2)	13.3(1)	.35	0.26(1)	.39	.05	.56
3.2	0.78	2.5	4.6(2)	.12	0.78(3)	5.5(2)	.16	10(2)	12.7(1)	.30	0.22(1)	.36	.07	.57
3.6	0.67	2.9	3.4(2)	.09	0.63(2)	4.1(1)	.12	10(2)	11.6(1)	.25	0.21(1)	.30	.06	.65
4.0	1.2	4.1	2.8(2)	.17	0.60(1)	-	-	-	10.9(1)	.24	0.21(1)	.26	-	.74
4.6	0.89	3.2	1.8(1)	.19	0.60(7)				9.7(1)	.19	0.21(1)	.18		.82
5.2	0.89	3.5	0.99(11)	.16	0.64(11)				8.7(1)	.17	0.19(1)	.11		.89
5.8	0.88	3.8	0.63(15)	.18	0.88(36)				8.0(1)	.15	0.18(1)	.08		.92
6.4	0.89	4.0	0.78(29)	.04	0.77(29)				7.3(1)	.14	0.17(1)	.05		.95
7.2	0.88	3.8	0.16(9)	.00	0.86(57)				6.5(1)	.13	0.15(1)	.02		.98
8.0	0.93	3.9	0.10	.15	0.99				5.9(1)	.12	0.13(1)	.02		.98

^a Obtained by a three-set (single-set) Debye model; χ in units of 10^{-6} m³ mol⁻¹; adiabatic susceptibility $\chi_s = 0$. $R(\chi')$ and $R(\chi'')$ – discrepancy factors of the fit. Standard deviation of the last digit in parentheses.

Slow magnetic relaxation in two mononuclear Mn(II) complexes not governed by the over-barrier Orbach process

R. Mičová, C. Rajnák, J. Titiš, E. Samoľová, M. Zalibera, A. Bieňko, R. Boča

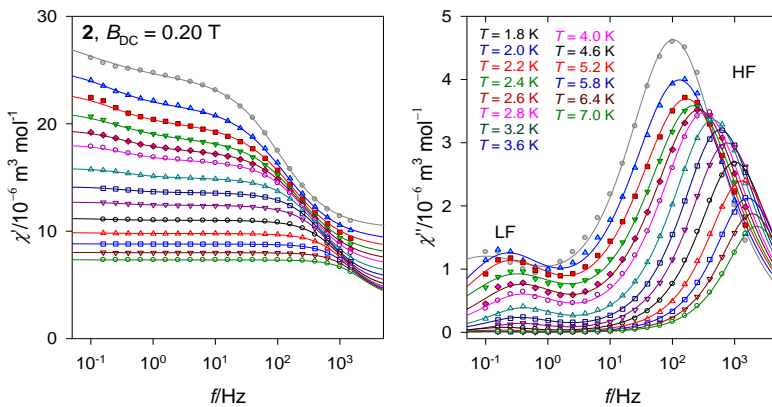


Figure S9. Frequency dependence of the AC susceptibility for **2**.

Table S6. Temperature dependence of AC susceptibility parameters for **2** at $B_{DC} = 0.2$ T.

T/K	$R(\chi')$ %/	$R(\chi'')$ %	χ_s	χ_{LF}	α_{LF}	τ_{LF} / s	χ_{HF}	α_{HF}	τ_{HF} /10 ⁻³ s	χ_{LF}	χ_{HF}
1.8	0.50	2.8	10.2(1)	14.9(13)	.43(9)	2.0	28.8(11)	.26(1)	1.51(3)	.25	.75
2.0	0.38	2.4	9.1(1)	14.3(9)	.46(6)	1.8(7)	26.6(8)	.28(1)	1.18(2)	.30	.70
2.2	0.71	2.2	8.3(1)	11.4(4)	.25(6)	0.71(11)	23.1(3)	.28(1)	0.94(2)	.21	.79
2.4	0.54	1.9	7.7(1)	10.4(3)	.30(6)	0.60(9)	21.3(2)	.26(1)	0.73(1)	.20	.80
2.6	0.42	2.1	7.1(1)	9.1(2)	.21(5)	0.48(5)	19.5(1)	.25(1)	0.60(1)	.16	.84
2.8	0.38	1.6	6.6(1)	8.2(1)	.19(1)	0.46(1)	18.1(1)	.22(1)	0.49(1)	.13	.87
3.2	0.24	1.0	5.9(1)	6.8(1)	.12(4)	0.43(3)	15.8(1)	.18(1)	0.36(1)	.09	.91
3.6	0.14	0.45	5.4(1)	6.0(1)	.10(4)	0.48(3)	14.1(1)	.15(1)	0.27(1)	.06	.94
4.0	0.21	0.97	5.0(1)	5.3(1)	.00	0.46(7)	12.7(1)	.13(1)	0.21(1)	.03	.97
4.6	0.19	1.4	4.6(1)	4.7(1)	.00	0.84(36)	11.2(1)	.11(1)	0.16(1)	.02	.98
5.2	0.17	1.6	4.3(1)	4.3(1)	.00	1.00	9.9(1)	.09(1)	0.12(1)	.01	.99
5.8	0.10	1.6	4.1(1)	4.1(1)	.00	1.75	8.8(1)	.07(1)	0.098(1)	.01	.99
6.4	0.12	0.89	4.0(1)	4.0(1)	.00	1.06	8.0(1)	.04(1)	0.083(1)	.01	.99
7.0	0.09	0.86	3.8(1)	3.8(1)	.00	1.25	7.3(1)	.03(1)	0.070(1)	0	1

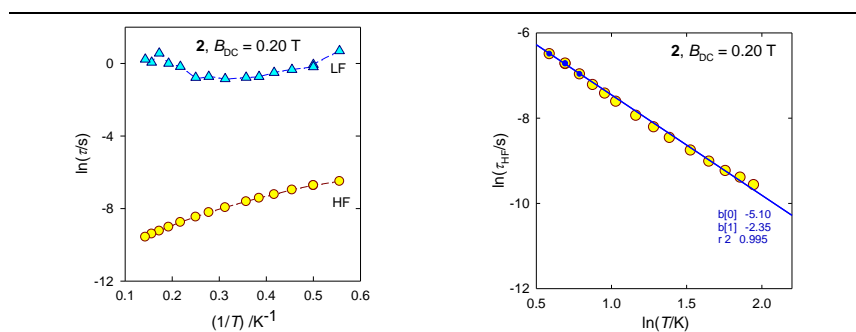


Figure S10. Temperature evolution of the relaxation time for **2**: left – Arrhenius like plot, right $\ln \tau$ vs $\ln T$ plot. Filled three low-temperature points were used in the linear regression according to $\ln \tau_{HF} = b_0 + b_1 \ln T = -\ln C - n \cdot \ln T$.

Slow magnetic relaxation in two mononuclear Mn(II) complexes not governed by the over-barrier Orbach process

R. Mičová, C. Rajnák, J. Titiš, E. Samoľová, M. Zalibera, A. Bieňko, R. Boča

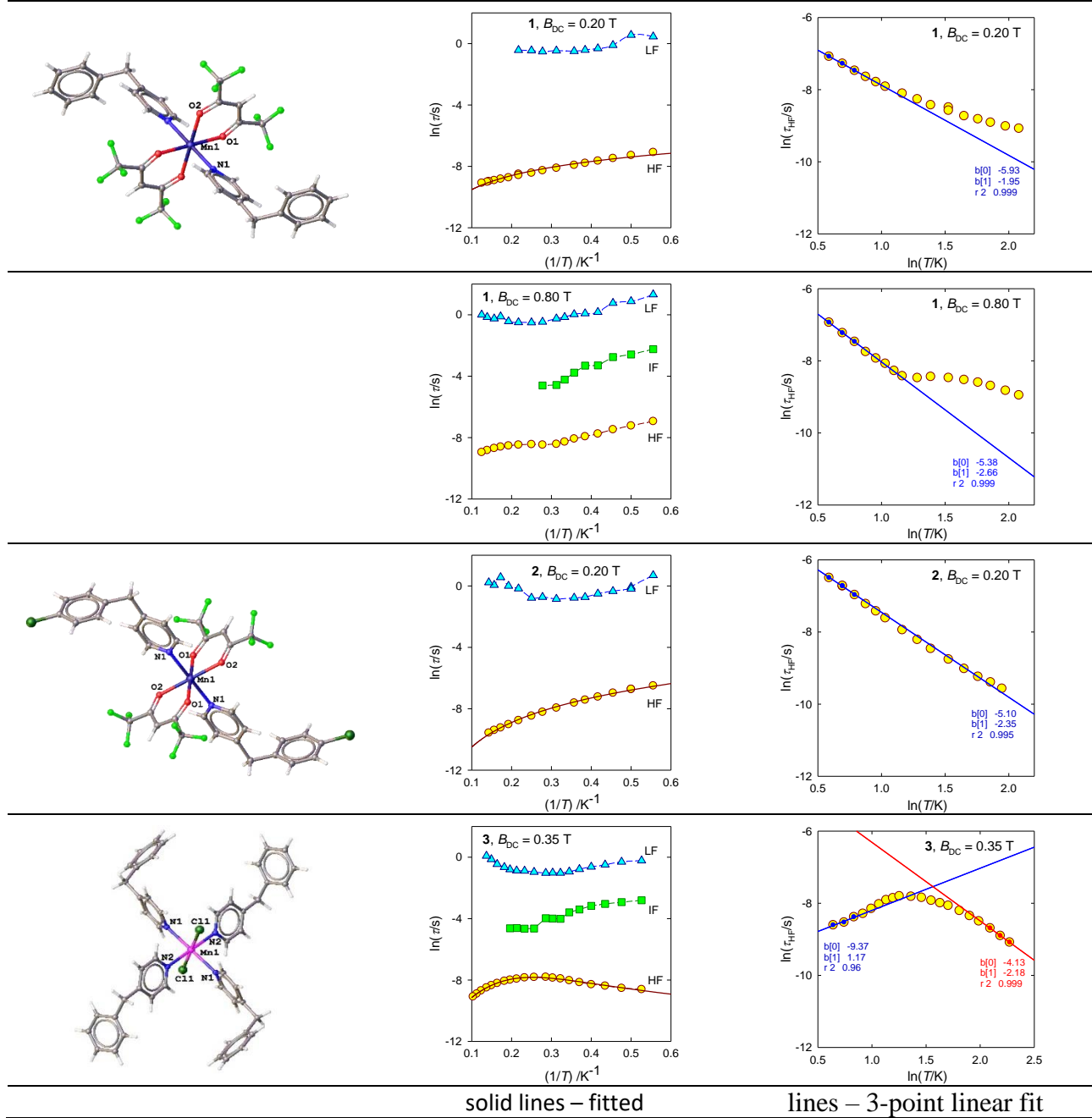


Figure S11. A comparison of the relaxation times for **1** through **3**. Data for **3** – Ref.⁵⁰ Findings:

- In **1** and **2** the low-temperature data (three points) can be fitted using eqn $\tau^{-1} = CT^n$ with the temperature coefficient $n = 1.95$ and $n = 2.35$ at $B_{DC} = 0.2$ T; $n = 2.66$ at $B_{DC} = 0.8$ T for **1**. This excludes the Raman and quantum tunneling mechanisms and approaches the direct relaxation mechanism ($n \sim 1$) or phonon bottleneck mechanism ($n \sim 2$). For **3** the unconventional relaxation was termed the *reciprocating thermal behaviour* for which on cooling the relaxation time is accelerated and the temperature coefficient is $n = -1.17$ close to the second solution for the phonon bottleneck process ($n \sim -1$).⁵⁰
- In **1**, the high-temperature data strongly deviate from the common relaxation types and the inverse relaxation time does not follow the T^n dependence.
- In **2**, the high-temperature data at $B_{DC} = 0.2$ T follow the behaviour of the low-temperature set with $n = 2.35$.
- In **3**, the high-temperature data can be fitted with $n = 2.18$ that again is far from the Raman or direct processes. In this case the complete data set can be fitted by using $\tau^{-1} = CT^n + FT^{-m}$.

Slow magnetic relaxation in two mononuclear Mn(II) complexes not governed by the over-barrier Orbach process

R. Mičová, C. Rajnák, J. Titiš, E. Samoľová, M. Zalibera, A. Bieńko, R. Boča

***Ab initio* calculations**

Table S7. Lowest sextet-to-quartet NEVPT2 transition energies and contributions to the *D*-tensor for **1** and **2**.

	1	2	
Root <i>i</i>	$\Delta E/\text{cm}^{-1}$	D_i/cm^{-1}	E_i/cm^{-1}
0	18299	-0.065	-0.314
1	18630	0.561	-0.115
2	19355	-0.423	0.418
3	23135	0.000	0.000
4	23806	0.000	0.000
5	24094	0.000	0.000
6	26339	0.000	0.000
7	26420	0.000	0.000
8	26598	0.000	0.000
9	28885	-0.001	-0.001
10	29270	0.000	0.000
11	29510	0.001	0.000
12	31988	-0.060	0.059
13	32192	-0.001	-0.002
14	36049	-0.437	-0.433
15	36244	-0.386	0.385
16	37027	0.845	0.000
17	43927	0.010	0.001
18	44149	-0.005	0.007
19	44493	-0.009	-0.010
20	45041	-0.002	0.001
21	48601	0.000	0.000
22	48642	0.000	0.000
23	49005	0.000	0.000

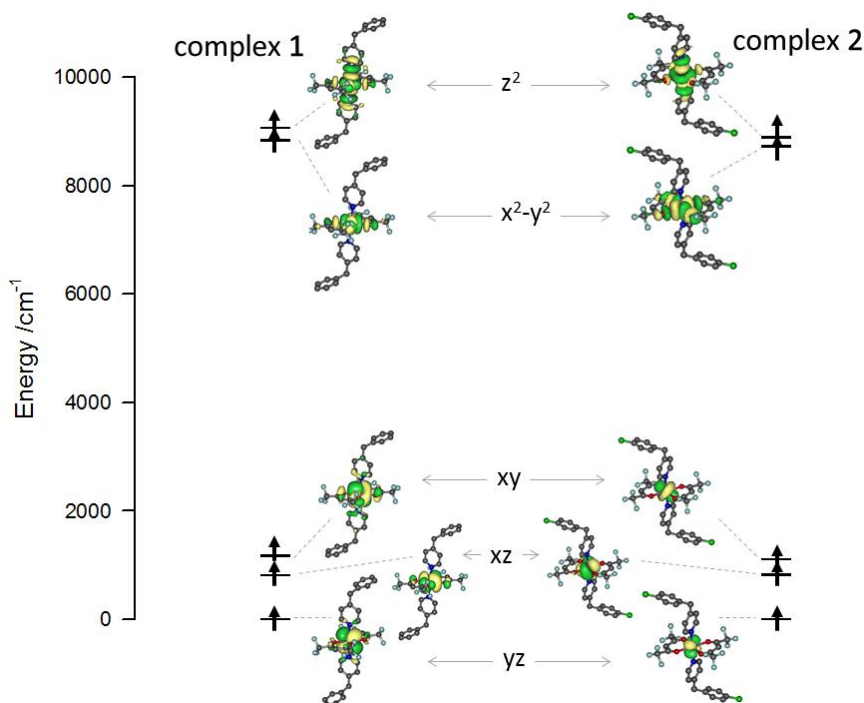


Figure S12. AI-LFT (*ab initio* ligand-field theory) relative energies of five singly occupied molecular orbitals for complexes under study (zoom for clarity).